SiF 2018– The 10th International Conference on Structures in Fire
FireSERT, Ulster University, Belfast, UK, June 6-8, 2018

INFLUENCE OF FIRE ON THE SHEAR CAPACITY OF STEEL-SHEATHED COLD-FORMED STEEL FRAMED SHEAR WALLS

Matthew S. Hoehler[1], Blanca Andres[2]

ABSTRACT

This paper discusses an experimental investigation of the influence of fire on the lateral load-carrying behaviour of steel-sheathed cold-formed steel framed shear walls. The completed Phase 1 tests showed an important example of structure-fire interaction and highlighted the relevance of the gypsum boards for both the thermal and mechanical behaviour of these systems. A second phase of the study is underway and is outlined in this paper with focus on the test program, specimen design and fire exposure development.

Keywords: cold-formed steel, fire, shear wall, steel-gypsum composite board

1 INTRODUCTION

Lightweight construction using cold-formed steel (CFS) studs represents roughly 20 % of the multi-story nonresidential building market in the United States [1]. These buildings rely on their lateral force-resisting systems (LFRS) to resist horizontal loads; e.g. from wind or earthquakes. While information exists about the structural performance and fire resistance of cold-formed steel construction; see for example [2–5], there is limited knowledge about the performance of CFS-LFRS under combined hazards. This information is needed to inform: (i) fire compartmentation design when significant lateral deformation of a building is anticipated, (ii) post-fire assessment of a structure, and (iii) first responder decisions to enter a building when earthquake aftershocks are likely.

In 2016, a series of experiments (Phase 1) was performed at the National Fire Research Laboratory at the National Institute of Standards and Technology (NIST) to investigate the performance of earthquake-damaged steel-sheathed cold-formed steel shear walls under fire load [6]. A second phase of the project currently underway (Phase 2) extends the study to two additional levels of fire severity and two additional types of CFS-LFRS. In this paper, the authors summarize key findings from Phase 1 and present the test program and setup for Phase 2; with focus on the steel-gypsum composite board assemblies. The Phase 2 experiments are being conducted at the time of writing this paper.

2 PHASE 1

The Phase 1 experiments were performed in conjunction with the project *Earthquake and Post-Earthquake Fire Performance of Mid-Rise Light-Gauge Cold-Formed Steel Framed Buildings* conducted at the University of California, San Diego (UCSD), which investigated the earthquake and fire performance of a six-story, cold-formed steel framed test building [7]. The NIST tests were conducted immediately prior to the six-story building tests to experimentally determine the influence

[1] Reserach Strucutral Engineer, National Institute of Standards and Technology, Gaithersburg, USA.
e-mail: matthew.hoehler@nist.gov
[2] PhD Student, Danish Institute of Fire and Security Technology, Hvidovre, Denmark.
e-mail: bav@dbi-net.dk

of the planned fires on the lateral load-resistance of the building to help inform the selection of the earthquake motion intensities used in the UCSD tests before and after the fires.

2.1 Test program and specimens

Table 1 shows the Phase 1 test matrix. Six identical 2.74 m by 3.66 m shear wall specimens were fabricated consisting of 150 mm wide CFS framing sheathed on one side with sheet steel adhered to 15.9 mm thick Type X (per [8]) gypsum board (Sure-Board 200[3]) and on the opposite side with 15.9 mm thick Type X gypsum board (*Fig. 1*). Fabrication details are provided in [6]. The specimens were subjected sequentially to varied combinations of mechanical (shear) deformation and thermal (fire) loading. Specimen 1 (CFS01) was used to establish the monotonic 'pushover' load-displacement response of the wall system. Specimen 2 (CFS02) was loaded by symmetric-amplitude reverse-cyclic shear deformation to destruction to establish the cyclic load-displacement response. Specimen 3 and 4 (CFS03 and CFS04) were cycled to deformations just before and after the peak load was achieved, respectively, burned for 13 min and 20 s and then cycling was continued until destruction of the wall. For Specimen 5 (CFS05), an undamaged wall was exposed to fire for 13 min and 20 s and then cycled to destruction. Specimen 6 (CFS06) was tested similarly to Specimen 3, however, the burn duration was doubled.

Table 1. Test matrix for Phase 1

Wall Type	Specimen Name	Loading		
		Before Fire	Fire	After Fire
Sure-Board	CFS01	Monotonic pushover	-	-
	CFS02	Cycle to failure	-	-
	CFS03	Cycle to 1 % drift	13 min 20 s burn	Cycle to failure
	CFS04	Cycle to 1.8 % drift	13 min 20 s burn	Cycle to failure
	CFS05	-	13 min 20 s burn	Cycle to failure
	CFS06	Cycle to 1 % drift	26 min 40 s burn	Cycle to failure

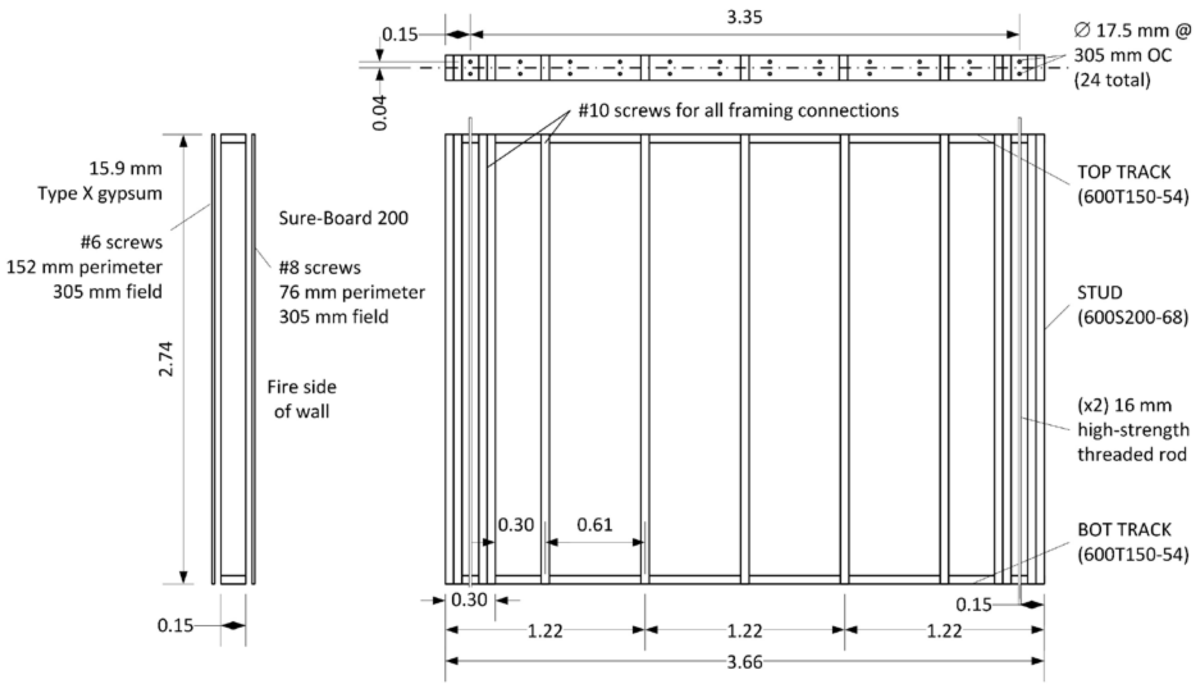

Fig. 1. Phase 1 specimen geometry (units in meters unless noted)

[3] Certain commercial products are identified in this paper to specify the materials used and the procedures employed. In no case does such identification imply endorsement or recommendation by the National Institute of Standards and Technology, nor does it indicate that the products are necessarily the best available for the purpose.

2.2 Test setup and procedure

The test setup was informed by ASTM E2126-11 [9] but deviated slightly to accommodate a burn compartment on a rolling platform. Details are provided in [6].

The test specimens were loaded mechanically by holding the base of the wall fixed and applying a prescribed in-plane deformation to the top of the wall as shown in *Fig. 2a*. Out-of-plane movement of the wall was limited by four structural steel guide frames. Mechanical load was applied using a servo-hydraulically controlled actuator with a load capacity of 240 kN in tension and 365 kN in compression. Axial loading to the wall was limited to the self-weight of the specimen, actuator and top loading beam. ASTM E2126-11 Method C (CUREE Basic Loading Protocol) was used with a reference deformation based on the expected deformation at peak load under monotonic loading. This protocol is widely used in the United States to characterize the seismic horizontal load resistance of vertical elements intended to form the lateral force resisting system in buildings. The loading procedure involved displacement cycles grouped in phases at incrementally increasing displacement levels. The rate of displacement was selected to be 1.52 mm/s to minimize inertial influences.

The fire load was provided by a natural gas diffusion burner in a compartment (interior dimensions: 2.9 m high × 3.5 m long × 1.2 m deep; see *Fig. 2b*) designed to approximate a portion of the corridor in the six-story building tested at UCSD. The open side of the compartment mated with the test specimen on the steel-gypsum composite board side of the shear wall. The openings at the ends of the compartment were 1.7 m high by 1.2 m wide. The mass flow rate of the natural gas was controlled to approximate the predicted time-temperature curves for upper gas layer temperatures in the 2nd floor corridor of the six-story building at UCSD during the fire tests. This was achieved by rapidly increasing (rise time less than 60 s) the Heat Release Rate (HRR) of the burner to 1900 kW and holding it constant for 800 s (13 min 20 s); for specimen CFS06 the burn duration was doubled. While the compartment temperatures rose more rapidly than for the standard fire curve in American Society of Testing and Materials (ASTM) standard E119 [10] (or International Organization for Standardization (ISO) standard ISO 834 [11]), they were representative of conditions present in residential fires in modern buildings [12]. The burn duration for the UCSD tests that the NIST tests were intended to simulate, was limited to about 15 minutes by the fire authorities in San Diego.

a)

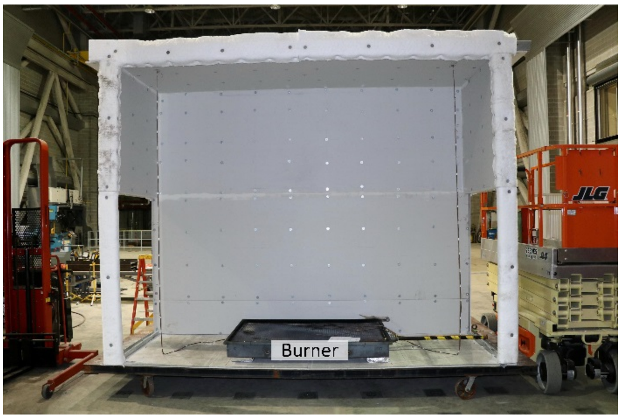

b)

Fig. 2. Photograph of test setups: a) Mechanical loading; b) Fire loading

2.3 Phase 1 results

The Phase 1 results are discussed in detail in [6,13] and data and videos can be downloaded at [14]. The uncertainties associated with all Phase 1 measurements are provided in [6]. The total expanded uncertainties (using a coverage factor of 2) associated with the forces and displacements reported in this paper are 1.6 kN and 2.3 mm, respectively.

Specimen 3 represents a typical loading case in Phase 1. The specimen was first cycled to a prescribed drift, subjected to fire load, and then, after the wall cooled, mechanical cycling was continued until the wall failed (defined as approximately 70 % reduction of post-peak load capacity). The resulting load-displacement curve is shown in *Fig. 3a*. The local maxima (load) for each step in the loading pattern are indicated for compression (circles) and tension (squares) excursions. The curves defined by these maxima show an abrupt reduction of force after the specimen was subjected to the fire.

The enveloping curves ('backbone') defined by the local maxima of applied force versus drift for the five cyclic tests are compared in *Fig. 3b*. Displacements (drifts) measured at the top of the specimens are converted to drift ratios by dividing by the specimen height (2.74 m). The portions of the curves indicated by dashed lines represent the mechanical response in the post-fire test. Test CFS02 represents the stiffness and capacity of the wall under ambient conditions. Test CFS05 represents the stiffness and capacity of the specimen after the steel-sheathed side has been subjected to the investigated fire load for 13 min 20 s. The reduction in peak load capacity was 35 % and the response was roughly symmetric for tension and compression cycles. The reduction in the peak load was accompanied by a shift in failure mode of the specimens from local buckling of the sheet steel (*Fig. 4a*) to global buckling of the sheet steel (*Fig. 4b*) for the unburned (CFS02) and burned (CFS05) walls, respectively. The fire severely damaged the gypsum on the burn side reducing the stiffness of the shear panels out-of-plane and creating a 15.9 mm standoff between the screw heads and the sheet steel; i.e. the thickness of the lost gypsum. This, in effect, transformed the specimen to a plain sheet steel shear wall with reduced constraint around the panel boundaries. Pre-damaging the specimen by reversed shear cycling to 1 % (CFS03) or 1.8 % (CFS04) drift ratio prior to the fire loading had no noticeable influence on the residual load bearing capacity of the wall. Doubling the burn time to 26 min 40 s (CFS06) caused additional reduction (approximately 15 %) of the post-fire lateral load bearing capacity due to the damage to the nonstructural gypsum board on the back side (cold side) of the wall during the longer burn; which was not present in the shorter tests.

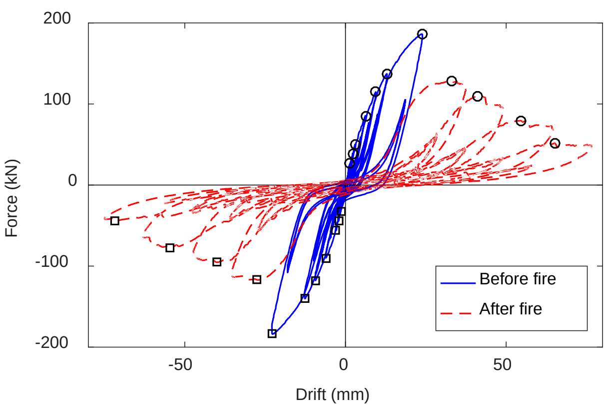

a)

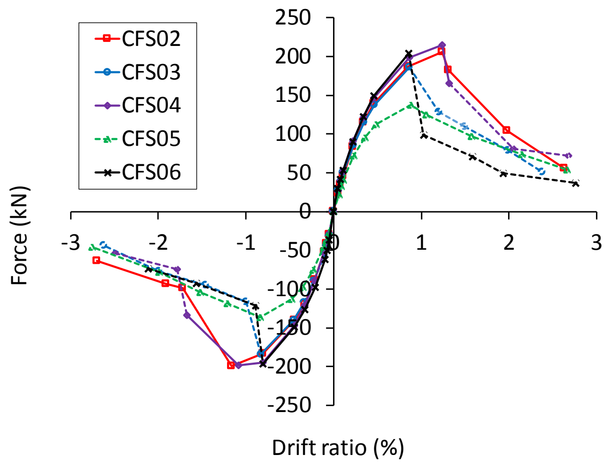

b)

Fig. 3. a) Lateral load versus drift for Specimen 3 (CFS03); b) Envelope force versus drift ratio curves for all cyclic tests (CFS02 to CFS06)

a) b)

Fig. 4. Photograph of back of sheathed side of wall with the nonstructural gypsum removed after mechanical loading to failure: a) Unburned wall after cycling (local buckling); b) Cycling after burning (global buckling)

3 PHASE 2

The Phase 1 experiments showed a clear example of structure-fire interaction (the shift in failure modes for the relatively short-duration fire) and highlighted the relevance of the gypsum for both the thermal and mechanical behaviour of these systems. Moreover, it appeared that this behaviour was predictable. This motivated the Phase 2 tests which include two additional types of CFS-LFRS, two additional levels of fire exposure, and locates the fire on the non-egress side of the shear wall.

3.1 Test program

Table 2 provides the test matrix for Phase 2. In addition to retesting the sheet steel adhered to Type X gypsum board (Sure-Board 200), Oriented Strand Board (OSB), and strap braced walls will be investigated. As in Phase 1, the walls are subjected to sequences of mechanical and fire loading. The test setup and mechanical loading procedure are the same as in Phase 1, however, the fire loadings differ as discussed below.

Table 2. Test matrix for Phase 2

Wall Type	**Specimen Name**	**Loading**		
		Before Fire	**Fire**	**After Fire**
Sure-Board	SB01	Cycle to failure	-	-
	SB02	-	ASTM E119 (1-hour)	Cycle to failure
	SB03	-	Severe Parametric	Cycle to failure
	SB04	-	Mild Parametric	Cycle to failure
OSB	OSB01	Cycle to failure	-	-
	OSB02	-	ASTM E119 (1-hour)	Cycle to failure
	OSB03	-	Severe Parametric	Cycle to failure
	OSB04	-	Mild Parametric	Cycle to failure
	OSB05	Drift Level 3	Severe Parametric	Cycle to failure
	OSB06	Drift Level 2	Severe Parametric	Cycle to failure
	OSB07	Drift Level 1	Severe Parametric	Cycle to failure
Strap braced	S01	Cycle to failure	-	-
	S02	-	ASTM E119 (1-hour)	Cycle to failure
	S03	-	Severe Parametric	Cycle to failure
	S04	-	Mild Parametric	Cycle to failure
	S05	Drift Level 3	Severe Parametric	Cycle to failure
	S06	Drift Level 2	Severe Parametric	Cycle to failure
	S07	Drift Level 1	Severe Parametric	Cycle to failure

Drift Level 1 = 0.5 %; Drift Level 2 = 1.0 %; Drift Level 3 = to be determined based on SB01, OSB01, and S01

3.2 Test specimen

The dimensioning of the walls is similar to Phase 1, however, the CFS framing design and tension holddowns are modified to be more representative of typical U.S. practice; the Phase 1 detailing focused on buildings with more than five storeys. The walls are designed using Allowable Stress Design (ASD) nominally following American Iron and Steel Institute (AISI) standards S400-15/S1-16 [15] and AISI S100-16 [16] assuming the walls are located on the interior of the building. The details for the gypsum and sheet-steel sheathed (Sure-Board 200) walls are shown in *Fig. 5*.

The walls are designed to achieve a 1-hour fire-resistance rating per ASTM E119 [10]. The design for fire-resistance of the steel-gypsum composite board walls is based on [17]. The walls use 15.9 mm thick Type X gypsum board with the joints taped and joints and fastener heads covered with one coat of joint compound on the fire side of the wall. The influence of insulation material in the wall cavity is not investigated.

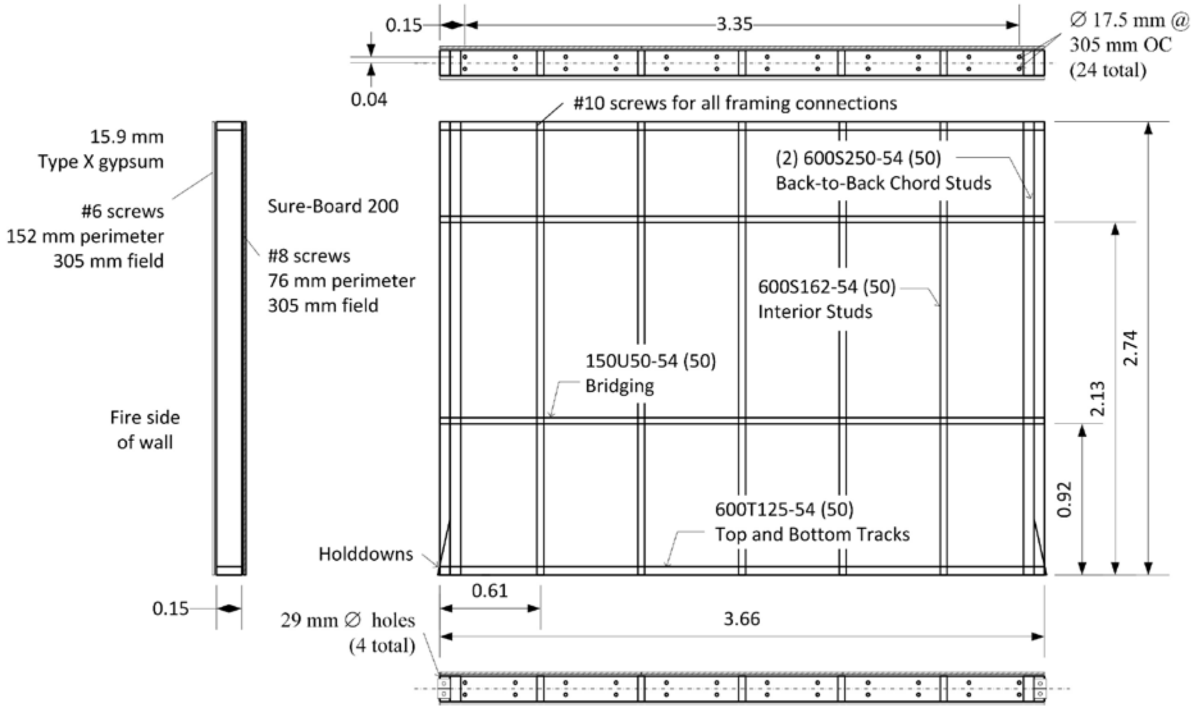

Fig. 5. Phase 2 steel-gypsum composite board specimen geometry (units in meters unless noted)

3.3 Fire load

The target fire exposures are selected to represent various levels of fire severity. Three exposures are considered in Phase 2: (1) a 1-hour standard ASTM E119 fire curve (comparable to ISO 834), (2) a 'severe' fire exposure, and (3) a 'mild' fire exposure. The severe and mild fires represent realistic post-flashover compartment fire conditions with heating, fully-developed and decay phases. *Fig. 6* plots the target temperature-time curves along with a typical upper layer gas temperature measured during Phase 1.

The severity of the fire is defined in terms of exposure time and peak temperature. These values are informed by a statistical fit of data from compartment fire tests reported by Hunt [18]. A peak temperature of 1100 °C represents 95 % of the reported peak temperatures and 900 °C represents 50 % assuming a normal distribution. These values were selected as the maximum temperatures for the 'severe' and 'mild' fires, respectively. Likewise, assuming a normal distribution of the duration of the fire, 70 minutes and 50 minutes represent 70 % and 50 % of the reported data, respectively.

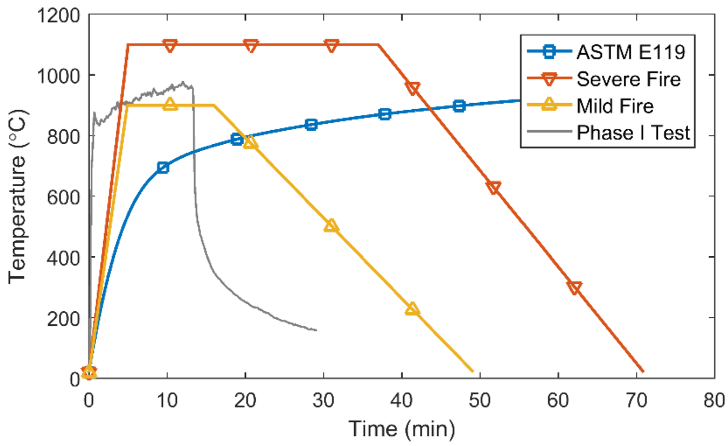

Fig. 6. Target temperature-time curves for Phase 2

The length of the plateau is calculated using the time-to-burnout for the enclosure fire (τ_b) per [18] and as given in *Eq. (1)*.

$$\tau_b = \frac{\mathrm{E} \cdot \mathrm{A}_f}{90\mathrm{A}_0\sqrt{H_0}} \text{ (minutes)} \tag{1}$$

where E is the fuel (energy) load per unit floor area of the enclosure (MJ/m²),
A_f is the floor area of the enclosure over which combustibles are present (m²),
A_0 is the opening area (m²), and
H_0 is the opening height (m).

In multi-unit residential buildings, shear walls are commonly located along corridors adjacent to a kitchen. Assuming a kitchen compartment and taking the mean values of floor area and fuel load density reported by the National Research Council Canada [19] for multi-family dwellings (9.8 m² floor area with 805 MJ/m²), opening factors[4] of 0.04 m$^{1/2}$ and 0.09 m$^{1/2}$ provide a time-to-burnout of 37 minutes and 16 minutes, respectively. These times defined the temperature plateaus for the 'severe' and 'mild' fires.

For comparison, the area under the target curve for the 'severe' fire represents a 20 % higher energy than ASTM E119 and the 'mild' fire corresponds to 40 % lower energy. The 'mild' fire is similar to the average upper gas layer time-temperature curves achieved in the Phase 1 tests.

4 SUMMARY

The results from Phase 1 indicate that a relatively short-duration (13 min 20 s) fire representative of modern furnished residential spaces acting directly on the shear panels caused a shift in the failure mode of the investigated steel-sheathed and gypsum shear walls under lateral loading from local to global bucking of the sheet steel with an accompanying reduction of the load capacity. The shear walls maintained a predictable, but reduced, lateral load capacity compared to ambient conditions. These observations prompted a second phase (Phase 2) of investigation described in this paper to extend the study to two additional shear wall systems and two additional fire loading exposures.

[4] Opening factor is defined as $\frac{\mathrm{A}_0\sqrt{H_0}}{\mathrm{A}_t}$, where A_o is the opening area (m^2), H_o is the opening height (m), and A_t is the area total enclosure (m^2).

ACKNOWLEDGEMENT

We thank Sure-Board, CEMCO, Marino/WARE, Panel Systems, Inc., Larry Williams, Benjamin Schafer, Rob Madsen, and the National Fire Research Laboratory staff for their expertise and support.

REFERENCES

[1] Steel Framing Industry Association, Market Share and Comparative Report: Cold-formed Steel Framing and Project Specification Trends, 2016.

[2] M.A. Sultan, A Model for Predicting Heat Transfer through Noninsulated Unloaded Steel-Stud Gypsum Board Wall Assemblies Exposed to Fire, Fire Technol. 32 (1996) 239–257.

[3] P. Keerthan, M. Mahendran, Numerical modelling of non-load-bearing light gauge cold-formed steel frame walls under fire conditions, J. Fire Sci. 30 (2012) 375–403. doi:10.1177/0734904112440688.

[4] H. Takeda, A model to predict fire resistance of non-load bearing wood-stud walls, Fire Mater. 27 (2003) 19–39. doi:10.1002/fam.816.

[5] X. Wang, E. Pantoli, T.C. Hutchinson, J.I. Restrepo, R.L. Wood, M.S. Hoehler, P. Grzesik, F.H. Sesma, Seismic Performance of Cold-Formed Steel Wall Systems in a Full-Scale Building, J. Struct. Eng. (United States). 141 (2015). doi:10.1061/(ASCE)ST.1943-541X.0001245.

[6] M.S. Hoehler, C.M. Smith, Influence of fire on the lateral load capacity of steel-sheathed cold-formed steel shear walls - report of test, Gaithersburg, MD, 2016. doi:10.6028/NIST.IR.8160.

[7] X. Wang, T.C. Hutchinson, G. Hegemier, S. Gunisetty, P. Kamath, B. Meacham, Earthquake and fire performance of a mid-rise cold-formed steel framed building – test program and test results: rapid release (preliminary) report (SSRP-2016/07), San Diego, CA, 2016.

[8] ASTM C1396-17 Standard Specification for Gypsum Board, ASTM International, West Conshohocken, PA, 2015. doi:10.1520/C1396.

[9] ASTM E2126-11 Standard Test Methods for Cyclic (Reversed) Load Test for Shear Resistance of Vertical Elements of the Lateral Force Resisting Systems for Buildings, ASTM International, West Conshohocken, PA, 2011. doi:10.1520/E2126-11.

[10] ASTM E119-16a Standard Test Methods for Fire Tests of Building Construction and Materials, ASTM International, West Conshohocken, PA, 2016. doi:10.1520/E0119.

[11] ISO 834-1 Fire Resistance Tests - Elements of Building Construction - Part 1: General Requirements, International Organization for Standardization, Genève, Switzerland, 1999.

[12] S. Kerber, Analysis of Changing Residential Fire Dynamics and Its Implications on Firefighter Operational Timeframes, Fire Technol. 48 (2012) 865–891. doi:10.1007/s10694-011-0249-2.

[13] M.S. Hoehler, C.M. Smith, T.C. Hutchinson, X. Wang, B.J. Meacham, P. Kamath, Behavior of steel-sheathed shear walls subjected to seismic and fire loads, Fire Saf. J. 91 (2017) 524–531. doi:10.1016/j.firesaf.2017.03.021.

[14] M.S. Hoehler, C.M. Smith, Dataset from Influence of Fire on the Lateral Resistance of Cold-Formed Steel Shear Walls - Phase I, (2018). doi:https://doi.org/10.18434/T4/1422515.

[15] AISI S400-15 w/S1-16, North American Standard for Seismic Design of Cold-Formed Steel Structural Systems (with Supplement 1), American Iron and Steel Institute (AISI), Washington, DC, 2016.

[16] AISI S100-16 North American Specification for the Design of Cold-Formed Steel Structural Members, American Iron and Steel Institute (AISI), Washington, DC, 2016.

[17] IAPMO-ER-1261 Sure-Board Series 200, 200W, and 200B Strucutral Panels Installed on Cold-Formed Steel or Wood Framed Shear Walls, International Association of Plumbing and Mechanical Officials (IAPMO), 2018.

[18] S.P. Hunt, J. Cutonilli, M. Hurley, Evaluation of Enclosure Temperature Emperical Models, Society of Fire Protection Engineers (SFPE), 2010.

[19] A.C. Bwalya, G.D. Lougheed, A. Kashef, H.H. Saber, Survey Results of Combustible Contents and Floor Areas in Multi-Family Dwellings, National Research Council Canada, 2008.